Aromatic Pathways in Conjugated Rings Connected by Single Bonds

3 AUTHORS, INCLUDING:

Stefan Taubert
University of Helsinki
17 PUBLICATIONS   **333** CITATIONS

SEE PROFILE

Dage Sundholm
University of Helsinki
205 PUBLICATIONS   **4,615** CITATIONS

SEE PROFILE

Aromatic Pathways in Conjugated Rings Connected by Single Bonds

STEFAN TAUBERT,[1] VILLE R. I. KAILA,[1,2] DAGE SUNDHOLM[1]

[1]*Department of Chemistry, University of Helsinki, P.O. Box 55 (A.I. Virtanens plats 1), FIN-00014 Helsinki, Finland*
[2]*Helsinki Bioenergetics Group, Structural Biology and Biophysics Programme, Institute of Biotechnology, University of Helsinki, P.O. Box 65, FIN-00014 Helsinki, Finland*

ABSTRACT: Magnetically induced current densities and molecular structures for molecules consisting of two conjugated rings formally connected by a single bond have been studied at correlated ab initio and density functional theory levels. The molecular structures and magnetically induced current densities were calculated for the lowest singlet and triplet states of biphenyl, bicyclobutadiene, phenyl-cyclobutadiene, and crosslinked phenol–imidazole, which is a model system for the crosslinked histidine–tyrosine found in heme–copper oxidases. Gauge-origin independent current densities were obtained by using the gauge-including magnetically induced current method. The lowest triplet states have a significantly shorter bond between the conjugated rings and generally a more planar structure when compared with the singlet ground state. The shorter bond distance between the conjugated rings indicates a π-electron delocalization between the rings. Current-density calculations show that the singlet states sustain ring currents mainly in the individual rings. The calculations also suggest that the shorter crosslink between the rings in the triplet states is accompanied with an increased current delocalization over the connected rings. © 2010 Wiley Periodicals, Inc. Int J Quantum Chem 111: 848–857, 2011

Key words: gauge-including magnetically induced currents; biphenyl; aromaticity; phenol-imidazole; open shell

1. Introduction

Planar conjugated molecular rings with $(4n+2)$ π-electrons are aromatic according to Hückel's rule [1, 2]. Molecules that are antiaromatic, i.e., comprising $(4n)$ π-electrons, have been suggested to show aromaticity in the lowest triplet state [3, 4]. The aromaticity criteria can analogously be applied to odd-electron systems such as radicals and radical anions [5, 6]. Anions of antiaromatic or nonaromatic neutral ring-shaped molecules with $(4n)$ π-electrons might be aromatically stabilized because the unpaired electron in the lowest unoccupied molecular orbital (LUMO) of the neutral system partially completes Hückel's rule.

Biphenyl consists of two rings with six π-electrons each, connected by a C–C single bond. The connected rings might be considered globally antiaromatic because of 12 π-electrons. Alternatively, biphenyl can be considered to consist of two unliked aromatic rings, as indicated by Hosoya [7]. Using graph theoretical arguments, Hosoya found that <5% of the aromaticity originates from a global picture [7]. Johansson and Olsen [8] recently studied biphenyl using coupled-cluster calculations at singles and doubles level including the standard triplet (CCSD(T)) correction [9, 10]. A structure with twisted arene rings was obtained in the calculations [8]. A very similar structure was obtained at the density functional theory (DFT) level using Becke's three-parameter functional [11] in combination with the Lee–Yang–Parr correlation functional [12] (B3LYP) as well as in second-order Møller-Plesset (MP2) calculations, suggesting that reliable structural information can be obtained at the B3LYP and MP2 levels for the molecules studied here.

Crosslinked aromatic moieties are also of crucial importance in many enzymes. For example, a histidine–tyrosine crosslink is a fully conserved structural motif among heme–copper oxidases [13–15]. The tyrosine presumably serves as both electron and proton donor in reduction of dioxygen to water within the active site of the enzyme [16]. Aromatic stabilization of the crosslinked histidine–tyrosine rings might be a reason for an increase of the electron affinity and a decrease of the proton affinity of the tyrosine moiety [17–19]. For obtaining a more complete picture of the aromatic character of connected conjugated rings, we investigate bond distances and current densities for molecules consisting of aromatic rings formally linked by a single bond. We also present results for molecules consisting of linked aromatic–antiaromatic rings as well as two linked antiaromatic rings. Biphenyl and the crosslinked phenol–imidazole species represent linked aromatic rings with 12 π-electrons. Bicyclobutadiene is an example of linked antiaromatic rings with eight π-electrons, and phenyl–cyclobutadiene represents crosslinked aromatic–antiaromatic species with 10 π-electrons.

Magnetically induced current densities are calculated using our gauge-including magnetically induced current (GIMIC) method [20]. The obtained current densities have no reference to the gauge origin because we use gauge-including atomic orbitals, also known as London atomic orbitals, in the current-density calculations [21–26]. The strength of the current passing selected chemical bonds is obtained by numerical integration of the current density passing through a plane perpendicularly to the investigated bond. The GIMIC method has previously been used in aromaticity studies of hydrocarbons [27–31], clusters [32–35], and hydrogen-bonded complexes [36]. The method has recently been extended for applications on open-shell species (Jusélius, Taubert, Sundholm, in preparation) rendering aromaticity studies on doublet, triplet, and higher multiplet states feasible.

2. Computational Methods

Molecular structures of the lowest singlet and triplet states of biphenyl, bicyclobutadiene, phenyl–cyclobutadiene, and crosslinked phenol–imidazole (2-imidazole-1-yl-4-methylphenol) species were optimized at the B3LYP and MP2 levels using the Karlsruhe def2-TZVP basis sets [37]. The resolution of the identity was used in the MP2 optimizations [38–40]. The molecular structure of neutral radical doublet state of the phenol–imidazole species was optimized at the same levels. For the open-shell molecules, the orbital contribution to the nuclear magnetic shielding constants (Jusélius, Taubert, Sundholm, in preparation) [41] was calculated at the MP2/def2-SVP and coupled-cluster singles and doubles (CCSD) levels using the CFOUR program [9, 42–44]. TURBOMOLE was used in the structure optimizations as well as in the magnetic shielding calculations on the closed-shell molecules [45–47]. The magnetically induced current densities were obtained using the GIMIC method. GIMIC is an independent program that uses basis-set information as well as the perturbed and unperturbed density matrices from nuclear magnetic shielding

TABLE I _____

The torsion angle (in degrees) between the rings and the length of the bridging bond (in pm) of the lowest singlet and triplet states, calculated at the B3LYP/def2-TZVP level.

	Torsion		Bond length	
Molecule	Singlet	Triplet	Singlet	Triplet
$(C_4H_3)_2$	0.0	0.0	138.4	133.5
$(C_6H_5)-(C_4H_3)$	0.0	0.0	143.7	141.9
$(C_6H_5)_2$	39.0	0.0	148.3	138.8
$(C_3N_2H_3)-(C_6H_4-OH)^a$	46.8	21.1	141.8	139.3
$(C_3N_2H_3)-(C_6H_5-O)^{-a}$	27.9	13.1	143.1	140.0
$(C_3N_2H_3)-(C_6H_4-O)^{a,b}$	27.1		139.4	

[a] Phenol-imidazole without the methyl group.
[b] Doublet.
The corresponding data for the doublet phenol–imidazole radical are also given.

TABLE II _____

The torsion angle (in degrees) between the rings and the length of the bridging bond (in pm) of the lowest singlet and triplet states, calculated at the MP2/def2-TZVP level.

	Torsion		Bond length	
Molecule	Singlet	Triplet	Singlet	Triplet
$(C_4H_3)_2$	0.0	0.0	136.6	134.2
$(C_6H_5)-(C_4H_3)$	0.0	0.0	143.5	145.3
$(C_6H_5)_2$	41.4	0.0	147.4	140.0
$(C_3N_2H_3)-(C_6H_4-OH)^a$	49.5		141.1	
$(C_3N_2H_3)-(C_6H_5-O)^{-a}$	32.5	15.9	142.3	141.0
$(C_3N_2H_3)-(C_6H_4-O)^{a,b}$	24.7		138.7	

[a] Phenol-imidazole without the methyl group.
[b] Doublet.
The corresponding data for the doublet phenol–imidazole radical are also given.

calculations as input data [20]. The GIMIC program is freely available on request from the authors. The current strengths (or actually the current susceptibilities) were obtained by numerical integration of the current densities passing selected chemical bonds. In the discussion, we use the term currents instead of current susceptibilities because the former is more intuitive. The two properties are linearly related by the strength of the external magnetic field.

3. Results and Discussion

The main structural features of the molecules consisting of two conjugated rings connected by a single bond are characterized by two parameters: the length of the bridging bond and the torsional angle between the two rings, given in Tables I and II. The molecules are depicted in Figure 1, and the atomic coordinates of the studied molecules are given as Supporting Information.

The strengths of the magnetically induced current passing the crosslink and around the rings of the studied molecules are summarized in Tables III–V. The current-density calculations including numerical integration of the current strengths show that electron-correlation effects are substantial for the open-shell molecules. For the triplet states, the current strengths calculated at the Hartree-Fock self-consistent field (HF-SCF) level are roughly one order of magnitude larger than those obtained at the MP2 and CCSD levels and will therefore not be discussed in this work.

3.1. BIPHENYL

The singlet ground state of biphenyl can be viewed as two arenes connected by a single bond. At the B3LYP/def2-TZVP level, the bond length is 147.4 pm, and the torsion angle between the phenyl
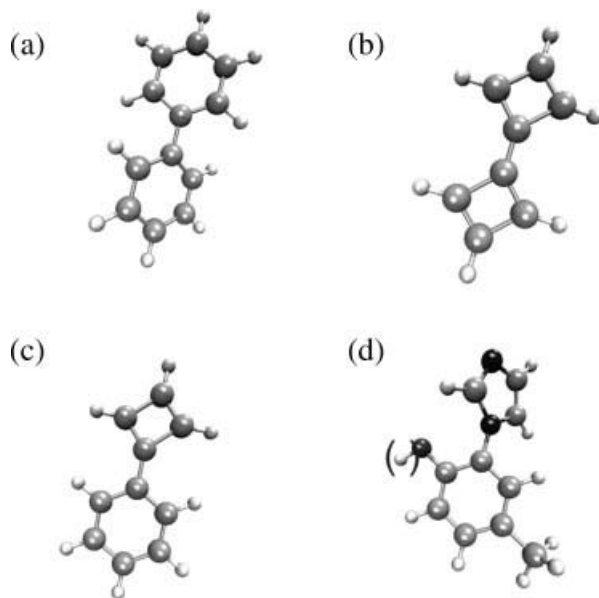

FIGURE 1. The molecular structures of the studied systems: (a) biphenyl, (b) bicyclobutadiene, (c) phenyl-cyclobutadiene, and (d) phenol–imidazole. The parenthesis indicates that the hydrogen is not present in the anion and the radical states. The molecular structures were visualized with VMD [48].

TABLE III

Magnetically induced current susceptibility strengths (in nA/T) through selected bonds in the lowest singlet state of the studied molecules.

Integration plane	A	B	C
$(C_4H_3)_2$		−17.0	8.6
$(C_6H_5)-(C_4H_3)$	10.8	−23.3	7.8
$(C_6H_5)_2$	11.5		7.2
$(C_3N_2H_3)-(C_6H_4-OH)$	10.2	8.2	7.4
$(C_3N_2H_3)-(C_6H_4-O)^-$	7.5	9.7	7.4
$(C_3N_2H_3)-(C_6H_4-O)^a$	8.1	6.5	8.3

[a] Doublet.

The current strengths of the neutral phenol–imidazole radical are also included. The current densities were obtained at the B3LYP/def2-TZVP level for the singlet and at the MP2/def2-SVP level for the doublet state of the radical. Cross section A is perpendicular to the outer bonds of the arene ring and the B plane is perpendicular to the outer bond of the other ring. C denotes the plane through half the bridging bond between the two rings.

rings is 39.0°. At the MP2 level, the obtained C–C bond length and torsion angle are 148.3 pm and 41.4°, respectively. Previous CCSD(T) calculations yielded a twist angle of 39° between the two phenyl rings [8]. The B3LYP and CCSD(T) angles are thus identical, whereas the experimental twisting angle is 44.4° ± 1.2° [8, 49]. The discrepancy between the CCSD(T) and experimental structures can be assigned to vibrational and temperature effects [8]. Experimentally, the planar and perpendicular orientations are transition states lying 6.0 ± 2.1 and 6.5 ± 2.0 kJ/mol higher in energy, respectively [50]. The

TABLE IV

Magnetically induced current susceptibility strengths (in nA/T) through selected bonds in the lowest triplet state of the studied molecules.

Integration plane	A	B	C
$(C_4H_3)_2$		−0.6	8.7
$(C_6H_5)-(C_4H_3)$	9.7	−2.5	5.1
$(C_6H_5)_2$	4.5		−10.9
$(C_3N_2H_3)-(C_6H_4-OH)$	9.2	2.7	7.2
$(C_3N_2H_3)-(C_6H_4-O)^-$	−15.5	8.1	−8.0

The current densities were calculated at the MP2/def2-SVP level using the B3LYP/def2-TZVP molecular structures. Cross section A is perpendicular to the outer bonds of the arene ring and the B plane is perpendicular to the outer bond of the other ring. C denotes the plane through half the bridging bond between the two rings.

TABLE V

Magnetically induced current susceptibility strengths (in nA/T) through selected bonds in the lowest triplet state of the studied molecules.

Integration plane	A	B	C
$(C_4H_3)_2$		−2.5	5.7
$(C_6H_5)-(C_4H_3)$	8.3	7.2	3.1
$(C_6H_5)_2$	1.8		2.0

The current densities were calculated at the CCSD/def2-SVP level using the B3LYP/def2-TZVP molecular structures. Cross section A is perpendicular to the outer bonds of the arene ring and the B plane is perpendicular to the outer bond of the cyclobutadienyl ring. C denotes the plane through half the bridging bond between the two rings.

experimental torsion barriers were largely reproduced by the CCSD(T) and B3LYP calculations in the complete basis-set limit by Johansson and Olsen [8].

The strength of the magnetically induced current passing an outer C–C bond of the phenyl rings 11.5 nA/T, i.e., practically the same as for benzene (11.8 nA/T) [31]. The calculations show that a current of 7.2 nA/T passes half the bridging C–C bond and returns on the other side of the C–C bond. The most obvious explanation is that the phenyl rings sustain ring currents of 11.5 nA/T implying that a bond current of 7.2 nA/T circles around the bridging C–C bond. Another equally plausible interpretation is that the phenyl rings sustain a ring current of 4.3 nA/T and a global current of 7.2 nA/T circles around the whole molecule. However, the current-density plot shown in Figure 2(a) supports the former interpretation, albeit any linear combination of the two interpretations is feasible.

Molecular structure optimizations of the first triplet state of biphenyl at the B3LYP and MP2 levels yield a planar structure with a significantly shorter C–C bond between the phenyl rings than for the singlet ground state. The C–C bond between the phenyl rings has a significant double-bond character, indicating that the system has a continuous electron delocalization pathway around both phenyl rings. The molecular structure calculations would thus suggest that the triplet state of biphenyl is globally aromatic rather than consisting of two connected but independent aromatic rings, which also Hückel's rule for the triplet state of a 12 π system suggests. The triplet state has a significant quinonoid character with large bond-length alternation and a continuous electron delocalization between the phenyl rings across the C–C bridge. At the MP2 level,
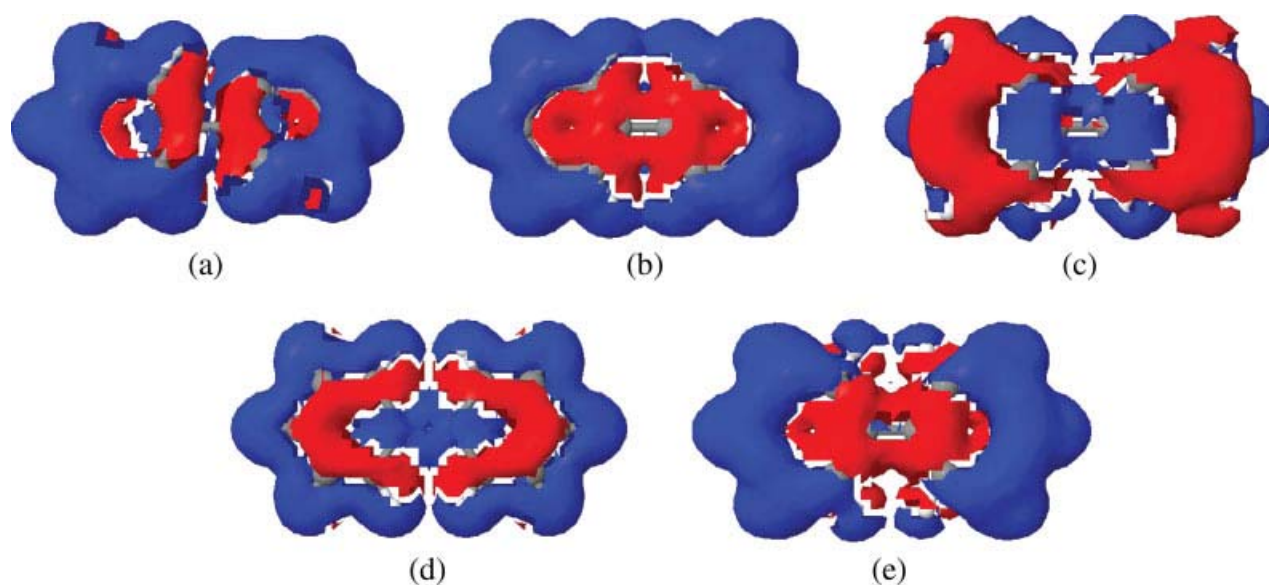
FIGURE 2. The current densities of biphenyl in the singlet ground state calculated at the B3LYP/def2-TZVP level (a). The current densities for the lowest triplet state were calculated at the MP2/def2-SVP level (b–e). The signed modulus of the charge and spin currents is depicted. (a) Total current of the singlet state, (b) total current of the triplet state, (c) spin current of the triplet, (d) the α contribution to the current, and (e) the β contribution to the current. An excess of α electrons is assumed for the triplet. The isocontour values for the densities are ± 0.005. The figure is plotted with JMOL [51]. [Color figure can be viewed in the online issue, which is available at wileyonlinelibrary.com.]

the C–C bridge is 140 pm, and the alternating double bonds are 134 pm. The single bonds next to the C–C bridge are 145 pm, and the outermost C–C bonds are 142 pm.

The MP2 current density of the first triplet state, shown in Figure 2(b), indicates that a diatropic ring current circles around the whole molecule. The diatropic current does not pass the C–C bond but flows instead through space between the hydrogens at the outer edge of the molecule, which also sustains strong paratropic currents inside the rings and between them. Integration of the current density passing the C–C bridge yields a paratropic current of $-10.9 \, \text{nA/T}$ at the MP2/def2-SVP level, whereas the ring current at the outer bonds of the phenyl rings is $4.5 \, \text{nA/T}$. The corresponding current strengths at the CCSD/def2-SVP level, summarized in Table V, are 2.0 and $1.8 \, \text{nA/T}$, respectively. Thus, the calculations at the CCSD level suggest that very weak diatropic currents dominate. According to the MP2 calculations, biphenyl is antiaromatic in the triplet state, whereas the CCSD calculations suggest a nonaromatic or a weakly aromatic biphenyl in the triplet state. The antiaromatic picture of the triplet biphenyl supports the obtained short C–C bond distance between the phenyl rings because previous calculations on [16] annulenes and expanded

porphyrins showed that antiaromatic molecules exhibit a smaller bond-length alternation when compared with nonaromatic molecules [52, 53].

Figures 2(d) and (e) show that diatropic currents, sustained by the α and β electrons, flow at the edge of the molecule around the entire molecule. A diatropic α current circles around the C–C crosslink, in addition to a delocalized paratropic current, which flows along the inside of the molecular framework. The spin currents calculated as the difference between the α and β currents are shown in Figure 2(c), assuming that the open-shell molecules have an excess of α electrons.

3.2. BICYCLOBUTADIENE

The planar bicyclobutadiene molecule consists of two cyclobutadienyl rings connected by a single C–C bond. At the B3LYP level, the molecule has a triplet ground state $77 \, \text{kJ/mol}$ below the closed-shell singlet state, whereas the MP2 calculations yield the opposite order of the singlet and the triplet states with the former $20 \, \text{kJ/mol}$ below the latter. The bridging C–C bond of the triplet state is 133.5 pm (134.2 pm at the MP2 level), whereas the B3LYP optimization yields a C–C distance of 138.4 pm (136.6 pm at the MP2 level)
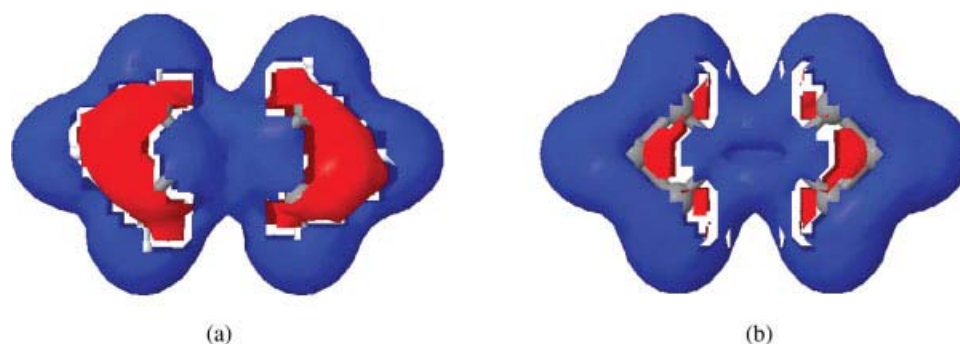
FIGURE 3. The signed modulus of the current densities of the lowest singlet and triplet states of bicyclobutadiene is depicted. The current densities were calculated at the B3LYP/def2-TZVP and MP2/def2-SVP levels for the singlet (a) and the triplet (b) states, respectively. The isocontour values for the densities are ± 0.005. The figure is plotted with JMOL [51]. [Color figure can be viewed in the online issue, which is available at wileyonlinelibrary.com.]

for the singlet state. The singlet and the triplet states are planar.

Because of its eight π-electrons, the singlet state of bicyclobutadiene can be considered to consist of two antiaromatic rings connected by a formal single bond. This is also supported by the current calculations, as a paratropic current strength of -17.0 nA/T was found to pass in the outer C–C bonds of the cyclobutadienyl rings. A diatropic current of 8.6 nA/T passes on one side of the bridging C–C bond and returns on the other side. An alternative interpretation is that a diatropic current of 8.6 nA/T is circling around both rings, and each cyclobutadienyl ring sustains paratropic ring currents of -25.6 nA/T. The current–density plot in Figure 3(a) supports the former interpretation.

For the triplet state, the strength of the current passing the outer C–C bonds of the cyclobutadienyl ring practically vanishes at the MP2 level. A strong diatropic current of 8.7 nA/T circles around the bridging C–C bond. An alternative interpretation involving a global diatropic ring current of 8.7 nA/T combined with local paratropic ring currents of -9.3 nA/T circling around the two cyclobutadienyl rings is less likely as indicated by the current density of the triplet state shown in Figure 3(b). The CCSD calculations yield qualitatively the same result with a paratropic current of -2.5 nA/T in the cyclobutadienyl ring and a current of 5.7 nA/T passing the C–C crosslink. Assuming that bicyclobutadiene has globally delocalized π-electrons, Hückel's rule suggests that the triplet state of the eight π system would be aromatic. However, the current-density calculations indicate that the cyclobutadienyl rings are weakly antiaromatic or nonaromatic.

3.3. PHENYL-CYCLOBUTADIENE

Phenyl-cyclobutadiene comprises a phenyl and a cyclobutadienyl ring, connected by a single C–C bond. For the singlet ground state, the two rings are separated by 143.7 pm at the B3LYP level, with a slightly shorter bond length of 141.9 pm obtained for the triplet state. In this case, both the singlet and the triplet states are planar. At the MP2 level, the C–C crosslink is 143.5 and 145.3 pm for the singlet and the triplet state, respectively.

For the singlet state, the current strengths obtained for the phenyl and cyclobutadienyl rings at the B3LYP level are typical for aromatic and antiaromatic molecules, respectively. The current strength of 10.8 nA/T in the phenyl ring is slightly weaker than for benzene, whereas the cyclobutadienyl ring sustains a paratropic ring current of -23.3 nA/T, which is somewhat stronger than for cyclobutadiene (-19.9 nA/T) [31]. A diatropic current of 7.8 nA/T passes the C–C crosslink. The alternative interpretation that 7.8 nA/T circles around the whole molecule yielding ring currents of 3 and -31.1 nA/T for the phenyl and cyclobutadienyl rings is less likely, as indicated by Figure 4.

Current calculations for the triplet state at the MP2 level yield a current strength of 9.7 nA/T in the outer C–C bonds of the phenyl ring and -2.5 nA/T in the outer cyclobutadienyl bonds. The current-density plots in Figures 4(a) and (b) indicate that the phenyl ring is aromatic, sustaining independent ring currents in both the singlet and the triplet states. A diatropic current of 5.1 nA/T circulating in the triplet state around the C–C crosslink. The corresponding current strengths obtained at the CCSD level are 8.3, 7.2, and 3.1 nA/T, thus suggesting that both rings
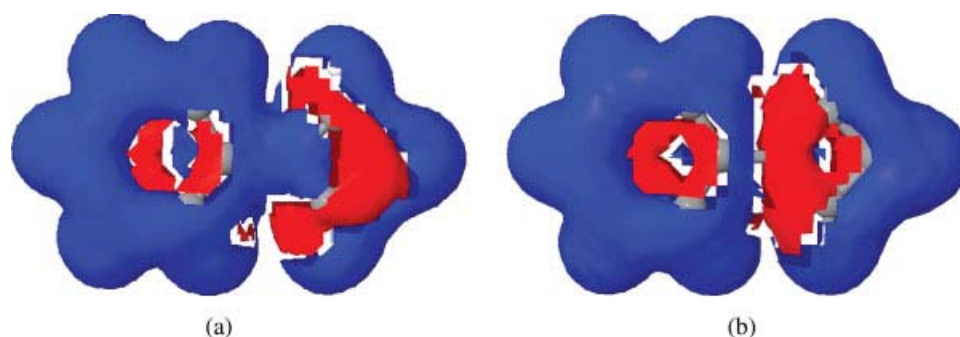
FIGURE 4. The signed modulus of the current densities of the lowest singlet and triplet states of phenyl-cyclobutadiene is depicted. The current densities were calculated at the B3LYP/def2-TZVP and MP2/def2-SVP levels for the singlet (a) and the triplet (b) states, respectively. The isocontour values for the densities are ±0.005. The figure is plotted with JMOL [51]. [Color figure can be viewed in the online issue, which is available at wileyonlinelibrary.com.]

are aromatic in the triplet state with a weak diatropic current of 3.1 nA/T passing the C–C bridge. This also correlates with the longer C–C bridge for the triplet state when compared with the singlet state. At the CCSD level, the cyclobutadienyl ring is aromatic because the exciton is mainly located in the cyclobutadienyl ring, which sustains a significant spin current of 6.0 nA/T when compared with −2.5 nA/T in the phenyl ring. Correlation effects are important for the relative energies of the phenyl-cyclobutadiene states. The singlet–triplet splitting is 132 kJ/mol at the MP2 level, whereas at the B3LYP level it is only 15 kJ/mol.

The current-density calculations at the CCSD level show that the triplet state of phenyl-cyclobutadiene comprises of two weakly coupled aromatic rings. Hückel's rule suggests that the triplet state of phenyl-cyclobutadiene with 10 π-electrons is a globally antiaromatic. Thus, the aromatic character of the connected phenyl and cyclobutadienyl rings cannot be judged merely from the total number of π-electrons.

3.4. PHENOL-IMIDAZOLE

3.4.1. Singlet and Radical Species

Abstraction of the phenolic proton and an electron from the crosslinked phenol–imidazole system taking place in the reaction cycle of cytochrome c oxidase (CcO) [16], which is a member of the heme–copper oxidase superfamily, decreases the torsion angle between the phenol ring and the imidazole from 46.8° to 27.1° and shortens the bridging bond by 2.4 to 139.4 pm at the B3LYP level. The subsequent reduction of the radical affects the torsion angle only

slightly, but the bridging C–N bond is stretched to 143.1 pm. Similar molecular structures are obtained at the MP2 level.

The current-density calculations yield very similar currents for the singlet state of neutral phenol–imidazole radical and the corresponding deprotonated anion. For the neutral singlet, the ring-current strength of the phenol ring is 10.2 or 2.0 nA/T stronger than for the imidazole ring. For the anion, the ring-current strength of the deprotonated phenol and imidazole rings is 7.5 and 9.7 nA/T, respectively. The bridging C–C bond has an edge current of 7.4 nA/T in these states. It remains elusive whether the edge current along the C–C bridge is a local bond current or a delocalized current around the entire molecule. However, the current-density plots in Figures 5(a) and (b) suggest that the two rings sustain independent ring currents.

The current density of the neutral phenol–imidazole radical is shown in Figure 5(c). Because of computational difficulties, the radical is represented by a model lacking the methyl group. Our calculations show that the methyl group has a negligible influence on the ring currents. For the radical, the current strength at the outer bonds of the phenol ring lies between the corresponding ring-current strength of the neutral protonated and the anionic deprotonated counterparts, whereas the current strength of 6.5 nA/T in the imidazole ring is weakest for the radical. The current across the bridge is 8.3 nA/T, i.e., 0.9 nA/T stronger in the phenol–imidazole radical than for the anionic singlet state, suggesting that the radical is somewhat stabilized by an increased electron delocalization. The difference cannot be explained by the shorter bridging bond in the radical when compared with the anion. For the
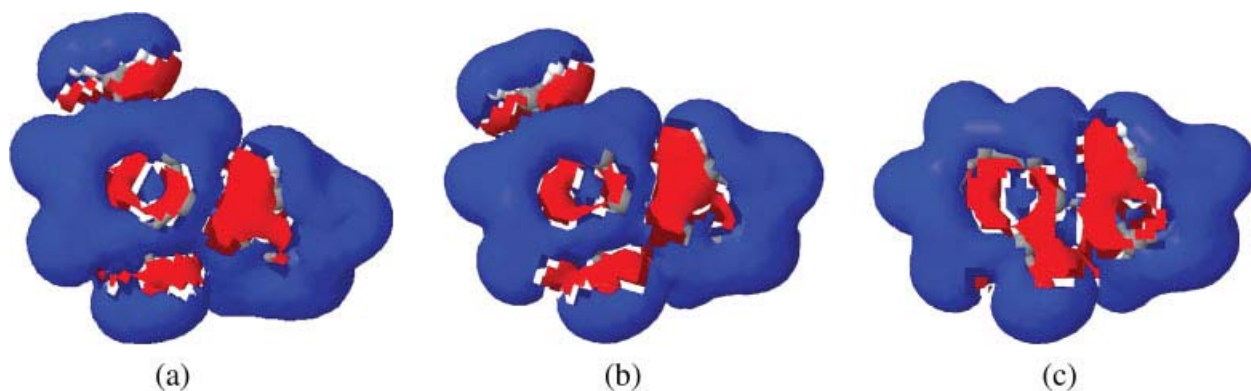
FIGURE 5. The signed modulus of the current densities of the lowest singlet states of crosslinked phenol–imidazole (a), its deprotonated anion (b), and for the doublet state of the neutral deprotonated phenol–imidazole radical (c) is depicted. The current densities were calculated at the B3LYP/def2-TZVP and MP2/def2-SVP levels for the singlet and the double states, respectively. The isocontour values for the densities are ±0.005. The figure is plotted with JMOL [51]. [Color figure can be viewed in the online issue, which is available at wileyonlinelibrary.com.]

phenol–imidazole anion, we studied the influence of the length of the bridging C–N bond on the current strength across the bridge. The current strength was calculated for structures with the C–N bond length varied in steps of 1 pm between 136 and 142 pm. The change in the current strength was only 0.15 nA/T in that interval. Thus, the increased current delocalization in the doublet phenol–imidazole cannot be explained by the C–N distance.

The strong current flow between the imidazole and phenol units in the crosslinked system might also be of biological relevance. The crosslinked phenol–imidazole (Tyr-244/His-240 according to bovine amino acid numbering) is a ligand of the redox active Cu_B center in heme–copper oxidases [13]. Reduction of the neutral phenol radical (Tyr-244) in the $P_M \rightarrow P_R$ transition of catalytic cycle of these enzymes couples to an increased proton affinity of the hydroxy ligand of the copper. According to present calculations, and previously observed in analysis of spin and charge densities of the system [18], the current flow between the rings is most probably of importance in establishing this nonlocal increase in proton affinity. Gorbikova et al. [54] recently observed that Tyr-244 is deprotonated in the first half of the catalytic cycle of CcO. Furthermore, Kaila et al. [18] described an electronic equilibrium between the copper and Tyr-244, when the former is deprotonated and the latter binds an aquo-ligand: Cu[II]/Tyr-O$^-$ $\leftrightarrow$ Cu[I]/Tyr-O*. The present calculations suggest that the aromatic coupling in the system might establish this resonance stabilization.

3.4.2. Triplet Species

The triplet states of phenol–imidazole and its deprotonated anion are not likely to have any relevance for biological applications, but they are included here for completeness. The B3LYP structures of the triplet states are more planar and possess a shorter bridging C–N bond than the singlet states. The torsion angle of the anion is reduced from 27.9° to 13.1°, and the bridging bond is compressed from 143.1 to 140.0 pm at the B3LYP level. The structure optimization of the triplet state of the neutral phenol–imidazole was unsuccessful at the MP2 level. The protonated neutral phenol–imidazole is more bent than the anion in the singlet state. In the first triplet state, the torsion angle is reduced by 25.7° to 21.1°, which is accompanied with a shortening of the C–N bond by 2.5 pm to 139.3 pm.

The current densities are shown in Figures 6(a) and (b), and current strengths are listed in Table IV. In the triplet state of phenol–imidazole, the two rings have slightly different aromatic character. The phenol ring has a ring current of 9.2 nA/T dominated by a diatropic current density on the outside, whereas the imidazole ring has a weaker ring current consisting of diatropic and paratropic contributions, adding up to a net current susceptibility of only 2.7 nA/T. Across the bridge, there is still a considerable current strength, which may be a superposition of a completely delocalized current loop and a local bond current of the bridging C–N bond, as discussed above.

For the anion, the triplet state sustains a strong paratropic current of −15.5 nA/T around the
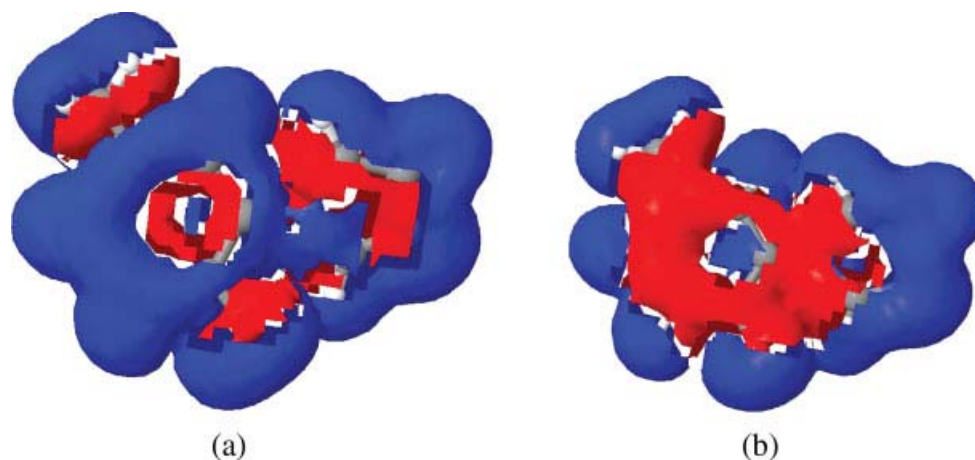
FIGURE 6. The signed modulus of the current densities of the lowest triplet states of crosslinked phenol–imidazole (a) and its deprotonated anion (b) is depicted. The current densities were calculated at the MP2/def2-SVP level. The isocontour values for the densities are ± 0.005. The figure is plotted with JMOL [51]. [Color figure can be viewed in the online issue, which is available at wileyonlinelibrary.com.]

phenol ring, whereas the net current of the imidazole is diatropic with a strength of 8.1 nA/T. The current passing the C–N crosslink is paratropic by -8.0 nA/T at the MP2 level. The current pattern of the triplet state of the phenol–imidazole anion is reminiscent to that of the triplet state of biphenyl.

4. Conclusions

The molecular structures of the lowest singlet and triplet states of biphenyl, bicyclobutadiene, phenyl-cyclobutadiene, and phenol–imidazole have been optimized at the B3LYP and MP2 levels. Current densities and strengths (susceptibilities) were investigated at the B3LYP level for the closed-shell systems and at the MP2 and CCSD levels for the open-shell species.

The singlet ground state of biphenyl and phenol–imidazole consists of two independent aromatic rings. The current-density calculations and molecular structure optimizations show that the bicyclobutadiene ground state comprises two antiaromatic rings connected by a single C–C bond, whereas the phenyl-cyclobutadiene ground state consists of an aromatic and an antiaromatic ring connected by a single C–C bond. The ground states of all studied molecules sustain significant bond currents along the crosslink. The current strengths of the phenol–imidazole radical are of the same magnitude as for the corresponding anion.

The current-density calculations show that electron-correlation effects are substantial for the open-shell molecules. The current strengths of the open-shell species calculated at the HF-SCF level are about one order of magnitude larger than those obtained at the MP2 and CCSD levels. For some of the studied systems, the current densities obtained at the MP2 and CCSD levels significantly differ. Current-density calculations at the MP2 level suggest that the triplet state of biphenyl is globally antiaromatic, whereas the CCSD calculations show that it is practically nonaromatic or possibly weakly aromatic. The triplet state of bicyclobutadiene sustains a weak paratropic current around the cyclobutadienyl rings and a diatropic current between the rings. At the MP2 level, the triplet state of phenyl-cyclobutadiene consists of an aromatic arene ring and an weakly antiaromatic cyclobutadienyl ring, whereas the CCSD calculations suggest that the two individual rings are aromatic. Both rings of the triplet states of neutral phenol–imidazole sustain diatropic currents at the MP2 level, whereas the triplet state of the phenol–imidazole anion has a similar current pattern as observed for biphenyl. Hückel's rule for triplet states cannot predict the aromatic character of all the investigated molecules.

References

1. Hückel, E. Grundzüge der Theorie Ungesättigter und Aromatischer Verbindungen; Verlag Chemie: Berlin, 1938.

2. von Eggers Doering, W.; Detert, F. L. J Am Chem Soc 1951, 73, 876.

3. Baird, N. C. J Am Chem Soc 1972, 94, 4941.

4. Gogonea, V.; von Ragué Schleyer, P.; Schreiner, P. R. Angew Chem Int Ed 1998, 37, 1945.

5. Vincow, G. Aromaticity, Pseudo-aromaticity, and Anti-aromaticity; Bergmann, E. D., Pullman, B., Eds.; Academic Press: New York, 1971; p 336.

6. Allen, A. D.; Tidwell, T. T. Chem Rev 2001, 101, 1333.

7. Hosoya, H. Monatsh Chem 2005, 136, 1037.

8. Johansson, M. P.; Olsen, J. J Chem Theory Comput 2008, 4, 1460.

9. Purvis, G. D.; Bartlett, R. J. J Chem Phys 1982, 76, 1910.

10. Raghavachari, K.; Trucks, G. W.; Pople, J. A.; Head-Gordon, M. Chem Phys Lett 1989, 157, 479.

11. Becke, A. D. J Chem Phys 1993, 98, 5648.

12. Lee, C.; Yang, W.; Parr, R. G. Phys Rev B 1988, 37, 785.

13. Yoshikawa, S.; Shinzawa-Itoh, K.; Nakashima, R.; Yaono, R.; Yamashita, E.; Inoue, N.; Yao, M.; Fei, M. J.; Libeu, C. P.; Mizushima, T.; Yamaguchi, H.; Tomizaki, T.; Tsukihara, T. Science 1998, 280, 1723.

14. Buse, G.; Soulimane, T.; Dewor, M.; Meyer, H. E.; Blüggel, M. Protein Sci 1999, 8, 985.

15. Rauhamäki, V.; Baumann, M.; Soliymani, R.; Puustinen, A.; Wikström, M. Proc Natl Acad Sci USA 2006, 103, 16135.

16. Proshlyakov, D. A.; Pressler, M. A.; DeMaso, C.; Leykam, J. F.; DeWitt, D. L.; Babcock, G. T. Science 2000, 290, 1588.

17. Bu, Y.; Cukier, R. I. J Phys Chem B 2005, 109, 22013.

18. Kaila, V. R. I.; Johansson, M. P.; Sundholm, D.; Laakkonen, L.; Wikström, M. Biochim Biophys Acta 2009, 1787, 221.

19. McCauley, M.; Vrtis, J. M.; Dupont, J.; van de Donk, W. A. J Am Chem Soc 2000, 122, 2403.

20. Jusélius, J.; Sundholm, D.; Gauss, J. J Chem Phys 2004, 121, 3952.

21. London, F. J Phys Radium 1937, 8, 397.

22. Hameka, H. F. Mol Phys 1958, 1, 203.

23. Ditchfield, R. Mol Phys 1974, 27, 789.

24. Wolinski, K.; Hinton, J. F.; Pulay, P. J Am Chem Soc 1990, 112, 8251.

25. Pulay, P.; Hinton, J. F.; Wolinski, K. Nuclear Magnetic Shieldings and Molecular Structure; NATO ASI Series C, Tossell, J. A., Ed.; Kluwer, 1993; vol. 386, p 243.

26. Gauss, J.; Stanton, J. F. Adv Chem Phys 2002, 123, 355.

27. Johansson, M. P.; Jusélius, J. Lett Org Chem 2005, 2, 469.

28. Jusélius, J.; Sundholm, D. Phys Chem Chem Phys 2008, 10, 6630.

29. Taubert, S.; Jusélius, J.; Sundholm, D.; Klopper, W.; Fliegl, H. J Phys Chem A 2008, 112, 13584.

30. Taubert, S.; Sundholm, D.; Pichierri, F. J Org Chem 2009, 74, 6495.

31. Fliegl, H.; Sundholm, D.; Taubert, S.; Jusélius, J.; Klopper, W. J Phys Chem A 2009, 113, 8668.

32. Lin, Y. C.; Jusélius, J.; Sundholm, D.; Gauss, J. J Chem Phys 2005, 122, 214308.

33. Johansson, M. P.; Jusélius, J.; Sundholm, D. Angew Chem Int Ed 2005, 44, 1843.

34. Lin, Y. C.; Sundholm, D.; Jusélius, J.; Cui, L. F.; Li, X.; Zhai, H. J.; Wang, L. S. J Phys Chem A 2006, 110, 4244.

35. Johansson, M. P. J Phys Chem C 2009, 113, 524.

36. Lin, Y. C.; Sundholm, D.; Jusélius, J. J Chem Theory Comput 2006, 2, 761.

37. Weigend, F.; Furche, F.; Ahlrichs, R. J Chem Phys 2003, 119, 12753.

38. Weigend, F.; Häser, M. Theor Chem Acc 1997, 97, 331.

39. Weigend, F.; Häser, M.; Patzelt, H.; Ahlrichs, R. Chem Phys Lett 1998, 294, 143.

40. Weigend, F.; Ahlrichs, R. Phys Chem Chem Phys 2005, 7, 3297.

41. Vaara, J. Phys Chem Chem Phys 2007, 9, 5399.

42. Stanton, J. F.; Gauss, J.; Harding, M. E.; Szalay, P. G. 2009. CFOUR, Coupled Cluster techniques for Computational Chemistry, a quantum-chemical program package also with contributions from Auer, A. A.; Bartlett, R. J.; Benedikt, U.; Berger, C.; Bernholdt, D. E.; Bomble, Y. J.; Christiansen, O.; Heckert, M.; Heun, O.; Huber, C.; Jagau, T.-C.; Jonsson, D.; Jusélius, J.; Klein, K.; Lauderdale, W. J.; Matthews, D. A.; Metzroth, T.; O'Neill, D. P.; Price, D. R.; Prochnow, E.; Ruud, K.; Schiffmann, F.; Stopkowicz, S.; Varner, M. E.; Vázquez, J.; Wang, F.; Watts, J. D. and the integral packages MOLECULE (Almlöf, J.; Taylor, P. R.); PROPS (Taylor, P. R.); ABACUS (Helgaker, T.; Jensen, H. J. Aa.; Jørgensen, P.; Olsen, J.); and ECP routines by Mitin, A. V.; van Wüllen, C. For the current version, see http://www.cfour.de.

43. Gauss, J. Chem Phys Lett 1992, 191, 614.

44. Gauss, J.; Stanton, J. F. J Chem Phys 1995, 102, 251.

45. Ahlrichs, R.; Bär, M.; Häser, M.; Horn, H.; Kölmel, C. Chem Phys Lett 1989, 162, 165; current version: see http://www.turbomole.com.

46. Kollwitz, M.; Gauss, J. Chem Phys Lett 1996, 260, 639.

47. Kollwitz, M.; Häser, M.; Gauss, J. J Chem Phys 1998, 108, 8295.

48. Humphrey, W.; Dalke, A.; Schulten, K. J Mol Graphics 1996, 14, 33.

49. Almenningen, A.; Bastiansen, O.; Fernholt, L.; Cyvin, B. N.; Cyvin, S. J.; Samdal, S. J Mol Struct 1985, 128, 59.

50. Bastiansen, O.; Samdal, S. J Mol Struct 1985, 128, 115.

51. JMOL: an open-source Java viewer for chemical structures in 3D. Available at: http://www.jmol.org.

52. Herges, R. Chem Rev 2006, 106, 4820.

53. Fliegl, H.; Sundholm, D.; Taubert, S.; Pichierri, F. J Phys Chem A, DOI 10.1021/jp1021517.

54. Gorbikova, E. A.; Wikström, M.; Verkhovsky, M. I. J Biol Chem 2008, 283, 34907.